Structures of magic Ba clusters and magic Ba suboxide clusters

Q. Wang, Q. Sun, J-Z. Yu, B-L. Gu,* and Y. Kawazoe
Institute for Materials Research, Tohoku University, Sendai 980-8577, Japan

Y. Hashi
Hitachi Tohoku Software Ltd., Sendai 980-0014, Japan
(Received 18 February 2000; published 13 November 2000)

Complementary to the experimental studies on magic Ba clusters [Rayane *et al.*, Phys. Rev. A **39**, 6056 (1989)], it is theoretically found that magic Ba clusters with 13, 19, 23, 26, 29, and 32 atoms have icosahedral or polyicosahedral structures, which are induced by $5d$-electron bonding. As the cluster grows, the average binding energy and mean bond length increase, while the highest occupied–lowest unoccupied molecular-orbital gap decreases. Due to the large atom size of Ba, there are large cavities in magic Ba clusters, where O atoms are trapped in the oxidation, and a small amount of oxygen can sustain the structural skeleton, which results in the fact that Ba suboxide clusters can have the same magic numbers as pure barium clusters, as found in experiment.

PACS number(s): 36.40.−c

I. INTRODUCTION

One of the significant goals in cluster science is to understand how physical properties and structures evolve from an atom to a molecule, to cluster, and in the end to a bulk phase. In this sense, divalent metal (Be, Mg, Ca, Sr, Ba) clusters are especially interesting systems. Due to the closed-shell ns^2 electronic configuration of their atoms, they can exhibit a nonmetal-metal transition as the cluster size increases. Their dimers are weakly bonded and as the cluster size increases, the valence s states hybridize with the unoccupied states, which leads to the metallization. Therefore, many studies were devoted to the divalent metal clusters. It has been found that the magic numbers for Be clusters are 4, 10, and 17 [1]. Larger Be clusters are based on a trigonal prism structure similar to the hcp bulk; Be_{13} is not an icosahedron, and there is a remarkable tendency toward two-dimensional growth pattern related to hcp packing, which suggests that directional bonding is important in these clusters [1].

For Mg clusters, tetrahedron and trigonal prisms are two important constituents of the structure to which atoms can be added by capping the faces [2], and the magic numbers are found to be 4 and 10 [2], which can be understood in terms of a filling of the electronic shells in a spherical jellium model [3]. For a Sr cluster, a recent experiment [4] found that the magic numbers are 11, 19, 23, 34, 43, 52, 61, and 81.

However, for a Ba cluster, the magic numbers are quite different. They are 13, 19, 23, 26, 29, and 32 [5], which are in agreement with the icosahedral sequence. In particular even after oxidation, the magic numbers do not change: $Ba_{13}O$, $Ba_{19}O$, and $Ba_{23}O$ are still magic [6]. Thus the following questions arise.

(1) Although the magic numbers for Ba clusters are the same as for the icosahedral sequence, do small Ba clusters really grow in an icosahedral pattern? Icosahedral growth in rare-gas clusters can be understood in terms of spherically symmetric pairwise interactions and a close packing of the Mackay icosahedral structures [7]. If small Ba clusters do grow in the icosahedral growth mode, what is the growth mechanism?

Although more than ten years have passed since the first identification of magic numbers for Ba clusters [5], no paper answering these questions has been published. As far as we know, only small Ba_n ($n=2-14$) clusters have been theoretically studied [8].

(2) In alkali-metal (Li, Na, Cs) oxide clusters [9–12], one oxygen atom localizes the valence electrons from two alkali-metal atoms; the remaining valence electrons from the other alkali-metal atoms are delocalized within the cluster, which can cause clusters to be magic in the form of $(M_2O)M_n$ with shell closings (e.g. $n=8$, 20, and 40 for Li; $n=8$, 18, 34, 58, and 92 for Cs). If this trend is followed in Ba oxide clusters, it seems that one oxygen atom should localize the valence electrons from one Ba atom, i.e. $(BaO)Ba_n$ should be magic, with $n=13$, 19, and 23. However, this conflicts with the experimental results. Why does oxidation not change the magic numbers? What is the role of the oxygen in the structure?

Theoretical studies concerning the above questions are highly desirable. In this paper we try to answer these questions by using first-principles methods.

II. THEORETICAL METHOD

Ab initio methods based on density-functional theory (DFT) are well established tools to study structural properties of materials. In particular the plane-wave basis and the pseudopotential method, combined with DFT, have provided a simple framework in which the calculation of Hellmann-Feynman forces is greatly simplified, so that extensive geometry optimization is possible. However, for oxygen, due to the lack of corresponding core states for cancellation, the tightly bound $2p$ valence wave functions are sharply peaked. As a result, in the conventional pseudopotential scheme, a

*Permanent address: Department of Physics, Tsinghua University, Beijing 100084, People's Republic of China.

relatively hard pseudopotential has to be generated, and a relatively large number of plane-wave basis functions are required in calculations, which causes some difficulties for studies of the structures of oxide clusters. In the present calculations, we used an *ab initio* ultrasoft pseudopotential scheme with a plane-wave basis (the Vienna *ab initio* simulation program) [13–15], in which the finite-temperature local-density functional theory developed by Mermin [16] is used, and the variational quantity is the electronic free energy. Finite temperature leads to a broadening of the one-electron levels that is very helpful for improving the convergence of Brillouin-zone integrations. The electron-ion interaction is described by a fully nonlocal optimized ultrasoft pseudopotential [13]. For oxygen, a $2s^2 2p^4$ configuration is used as the reference state to construct ultrasoft pseudopotentials; for *s* and *p* orbitals, the cutoff radii are 1.40 and 1.55 a.u., respectively. With this ultrasoft pseudopotential, for the O_2 molecule, a bond length of 1.21 Å is obtained, which is in good agreement with the experimental value of 1.207 Å [17]. For an H_2O molecule, the H-O bond length is 0.963 Å and the $\angle$H—O—H bonding angle is 104.9°, also in agreement with experimental results of 0.9575 Å and 104.51° [17].

A minimization of the free energy over the electronic and ionic degrees of freedom is performed using the conjugate-gradient iterative minimization technique [18]. In the optimizations of structures, the edge lengths chosen for the supercubic cell are 33 and 22 Å for pure Ba clusters and small Ba oxide clusters, respectively. In such a large supercell, we use the Γ point to represent the Brillouin zone. The exchange-correlation energy of valence electrons is adopted from the form of Ceperley and Alder [19] as parametrized by Perdew and Zunger [20]. The structure optimization is symmetry unrestricted, and the optimization is terminated when all the forces acting on the atoms are less than 0.03 eV/Å.

III. RESULTS AND DISCUSSIONS

In order to test our calculations, first we have performed numerical calculations on Ba_2, Ba_4, and BaO. The obtained bond length for Ba_2 is 4.72 Å; for Ba_4 the most stable structure is a regular tetrahedron with a bond length of 4.44 Å, and for BaO the bond length is 2.09 Å. All of these are in agreement with the other theoretical results [6,8].

A. Structures and growth mechanism of magic Ba clusters

1. Structures

To confirm whether small Ba clusters really grow in an icosahedron sequence, we choose several structures to calculate: polyicosahedral structures [7] with 13, 19, 23, 26, 29, and 32 atoms, such that the center(s) of the icosahedral form(s) a monomer, a dimer, an equilateral triangle, a tetrahedron, a trigonal bipyramid, and so on; for some clusters, the calculations are also performed on other structures, as listed in Table I. For Ba_{13} and Ba_{19} clusters, a polyicosahedron (PICO), a decahedron (DEC), and a cuboctahedron are calculated. For a Ba_{23} cluster, a polyicosahedron and a decahedron are calculated. For a Ba_{32} cluster, four structures are calculated. The first one is polyicosahedron. The second one also has an icosahedral symmetry structure, composed of two concentric spherical shells: the inner shell is an icosahedron, and the outer shell is a dodecahedron, having 12 and 20 atoms, respectively. The third structure is a Bergman sphere [21], which exchanges the inner and outer shells in the second structure. The fourth structure has a D_{4h} symmetry formed of six squares and eight centered hexagons, and is the most stable of the spherical structures of the B_{32} cluster [22]. Comparing the average binding energy per atom, we find that, among all the isomers, the polyicosahedral structure is most stable, which should be also true for Ba_{26} and Ba_{29} clusters from the general trend, although only a PICO structure is calculated for these two clusters. Figure 1 shows the structures of the calculated clusters. Figure 2 shows the changes of the average binding energy per atom ϵ, and a highest occupied–lowest unoccupied molecular-orbital (HOMO-LUMO) gap δ, and the mean nearest-neighbor bond length *r* with the cluster size for PICO structures. We see that with the increase of cluster size the average binding energy per atom increases. However, a small oscillation exists for a Ba_{32} cluster: the binding energy is a slightly smaller as compared to that for Ba_{29}. The HOMO-LUMO gap decreases rapidly with the cluster size. In clusters, the contraction of the bond length is believed to be a reflection of the surface effect; as the cluster grows, the mean nearest-neighbor bond length *r* increases, as indicated in Fig. 2(c).

TABLE I. Mean nearest-neighbor bond length r(Å), total binding energy E (eV), the average binding energy per atom ϵ (eV), and the HOMO-LUMO gap δ (eV) for several structures: icosahedron (ICO), decahedron (DEC), cuboctahedron (CUB), polyicosahedron (PICO), and Bergman sphere (BS).

Cluster	Isomer	r	E	ϵ	δ
Ba_{13}	ICO	4.289	16.0511	1.2347	0.5885
	DEC		14.5379	1.1183	0.0694
	CUB		13.7176	1.0552	0.0020
Ba_{19}	PICO	4.320	24.6430	1.2970	0.2821
	DEC		22.5055	1.1845	0.2010
	CUB		21.6315	1.1385	0.2000
Ba_{23}	PICO	4.340	30.6130	1.3310	0.1505
	DEC		28.1175	1.2225	0.1100
Ba_{26}	PICO	4.342	31.0707	1.3509	0.1497
Ba_{29}	PICO	4.345	39.4400	1.3600	0.1400
Ba_{32}	PICO	4.406	43.3280	1.3540	0.0540
	IH		42.2272	1.3196	0.0010
	BS		34.6560	1.0830	0.0020
	D_{4h}		36.7104	1.1472	0.0139

2. Growth mechanism

As stated above, small Ba clusters grow in an icosahedral sequence. Why is this? Up to now, it was found that there are two kinds of clusters growing in an icosahedral mode: one is

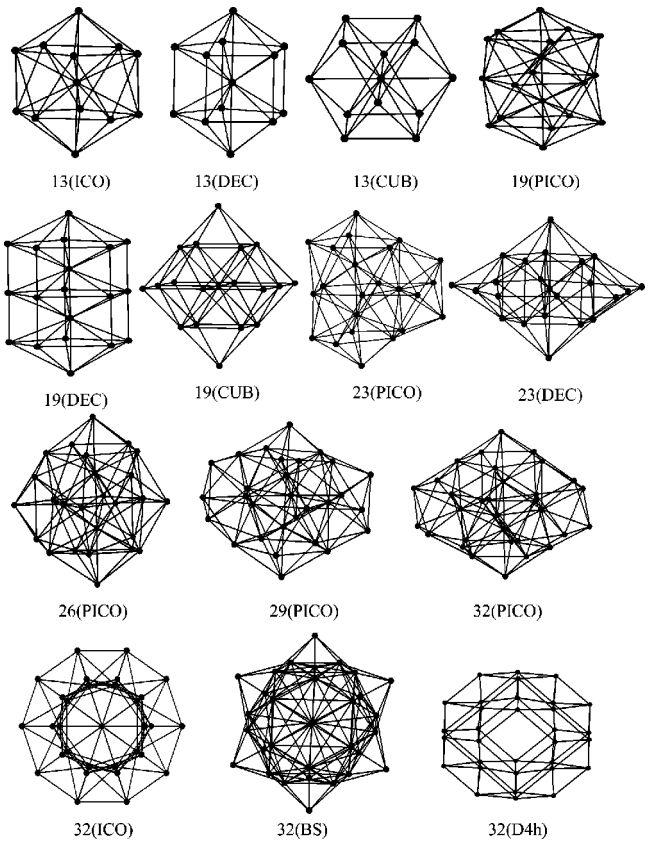

FIG. 1. Calculated structures for Ba_n clusters ($n=13$, 19, 23, 26, 29, and 32) with some isomers: icosahedron (ICO), decahedron (DEC), cuboctahedron (CUB), polyicosahedron (PICO), Bergman sphere (BS), and D_{4h} symmetry structure ($D4h$).

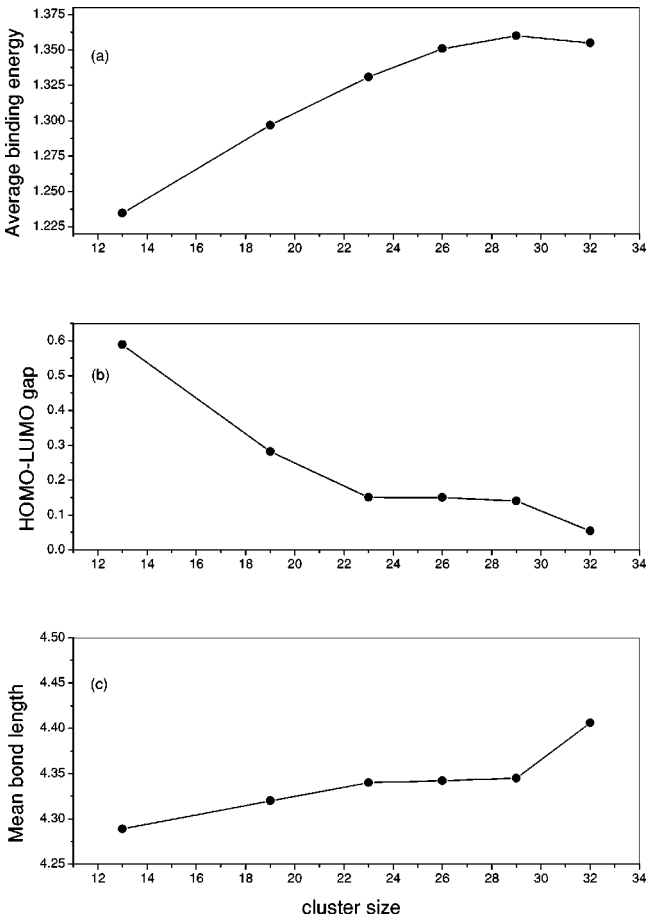

FIG. 2. Average binding energy (eV), HOMO-LUMO gap (eV), and mean bonding length (Å) as functions of cluster size for polyicosahedral structures, where the points are connected to aid the eye.

a rare-gas cluster which can be understood in terms of spherically symmetric pairwise interactions and a close packing of the Mackay icosahedral structures [7]. Another is a transition-metal cluster: experiments on Ni clusters provided indirect evidence of icosahedral growth [23], while enhanced stability was found for icosahedral structures of Ni_n clusters with $n=13$, 19, 23, and 26, by using the embedded-atom method [24]. A recent experiment on Fe clusters provided clear evidence of icosahedral growth with magic numbers of 13, 19, and 23 [25]. In the case of Ba clusters, the bonding features are naturally different from those of rare-gas clusters, but have one feature in common with Fe and Ni clusters: *d* electrons participate in the bonding. A Ba atom has a $6s^2$ closed-shell configuration, and low-lying empty $5d$ and $6p$ shells; the ground state is $6s^2$ ($^1S_0$), while its first excited state is $6s^15d^1$ ($^1D_1$). Therefore, in Ba clusters, due to the orbital hybridization, $5d$ electrons are expected to contribute to the bonding, which can be detected by Mulliken population analysis. To this end, with the optimized structure, numerical atomic wave functions are used as the basis set for the expansion of wave functions. Group theory is used to symmetrize the basis functions, which transforms as one of the irreducible representations of the point group of the cluster [26]. The $5d$, $6s$, and $6p$ orbitals of Ba are used as the basis set, and the cluster orbitals are expanded in a linear combination of the symmetrized basis functions. The Kohn-Sham equation is solved self-consistently with the discrete variational method [27].

Ba_{13} and Ba_{19} are taken as examples of Mulliken population analysis. For a Ba_{13} cluster, the average Mulliken populations per atom in $5d$, $6s$, and $6p$ orbitals are 0.7794, 0.6865, and 0.5226; while for a Ba_{19} cluster, the corresponding numbers are 0.7929, 0.7770, and 0.4300, respectively. Furthermore, the HOMO in Ba_{13} is composed of 79% $5d$, 19% $6s$, and 2% $6p$ orbitals. The HOMO in Ba_{19} is composed of 71% $5d$, 22% $6s$, and 7% $6p$ orbitals, as indicated in Table II. We can see that $6s$ orbitals strongly hybridize with $5d$ and $6p$ orbitals, differing from the situations in Be and Mg clusters [1,2], where only sp hybridizations

TABLE II. Average Mulliken population and orbital components (%) of the HOMO for Ba_{13} and Ba_{19} clusters.

Cluster	Average Mulliken population			HOMO		
	$5d$	$6s$	$6p$	$5d$	$6s$	$6p$
Ba_{13}	0.7794	0.6865	0.5226	79.0	19.0	2.0
Ba_{19}	0.7929	0.7770	0.4300	71.0	22.0	7.0

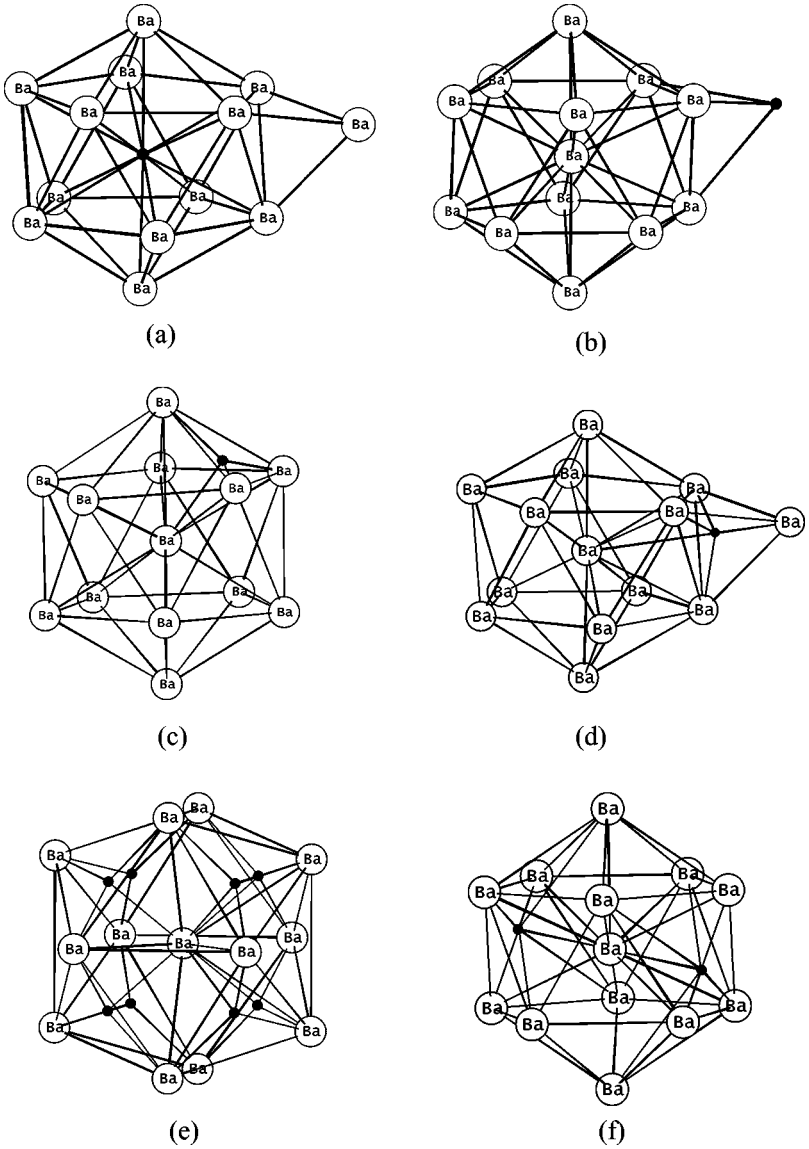

FIG. 3. Structures for (a)–(c) $Ba_{13}O$, (d) $Ba_{14}O$, (e) $Ba_{13}O_8$, and (f) $Ba_{13}O_2$ clusters, where the small black ball stands for the O atom.

exist, resulting in different magic numbers. $5d$ electrons in Ba clusters contribute considerably to the bonding, which causes small Ba clusters to grow in an icosahedral mode.

B. Stability of Ba oxide cluster

As mentioned in Sec. I, experiments show that $Ba_{13}O$, $Ba_{19}O$, and $Ba_{23}O$ clusters are magic, while $(BaO)Ba_n$ clusters ($n=13$, 19, and 23) are not, Why is this? Due to limited computer memory, we focus mainly on $Ba_{13}O$ and $(BaO)Ba_{13}$ clusters, which can shed some light on this question.

In a $Ba_{13}O$ cluster, where should the O atom be trapped? We have compared several configurations: (1) The O atom substitutes for the central Ba atom, which is capped on the threefold site of the icosahedron $Ba_{12}O$, forming a $(Ba_{12}O)Ba$ cluster [shown in Fig. 3(a)]. (2) The O atom is capped on the threefold site of the icosahedron Ba_{13} forming a $Ba_{13}O$ cluster [Fig. 3(b)]. (3) The O atom is in the interstitial site of a Ba_{13} cluster [Fig. 3(c)]. It is found that the last situation is the most stable. The average binding energy per atom is 2.13 eV, and the mean nearest bond length among Ba atoms decreases to 4.254 from 4.289 Å for a pure Ba_{13} cluster.

According to the icosahedron growth mode, the structure of Ba_{14} is a capped icosahedron. Among all possible configurations, we found that the most stable position for an O atom in Ba_{14} is that the O atom is inside of a tetrahedron composed of the capped Ba atom and three surface Ba atoms shown in Fig. 3(d). The average binding energy per atom in this cluster is 2.04 eV, which is smaller than that for a $Ba_{13}O$ cluster, suggesting that a $Ba_{13}O$ cluster is more stable than a $(BaO)Ba_{13}$ cluster. This is the reason that a $Ba_{13}O$ cluster is observed in mass spectra and a $(BaO)Ba_{13}$ cluster is not. Why does oxidation not change the magic numbers? From the structure of the $Ba_{13}O$ cluster, we found that there is a large cavity; the mean bond length of Ba-O is 2.545 Å, which is much larger than the bond length in a BaO molecule. Due to the high stability of Ba_{13}, the absorbed oxygen is trapped in the large cavity. Due to the bonding of $5d$ electrons, the jellium model is not valid for a Ba cluster;

accordingly, the situation in Ba oxide clusters is different from that of alkali-metal oxide clusters, where one oxygen atom localizes the valence electrons from two alkali-metal atoms, and the remaining valence electrons from the other alkali-metal atoms are *still* delocalized to form a jellium sphere [9–12].

In order to explain the changes in the ionization potential of a barium suboxide cluster, the authors of Ref. [6] proposed the following idea: the bare cluster Ba_{13} is a regular icosahedron, in which the 20 triangles on the surface and the central Ba atom consist of 20 tetrahedrons. If the possibility for an oxygen-containing tetrahedron sharing one face is excluded, there are altogether eight nonadjacent tetrahedrons, which means that the maximum number for O atoms included in a Ba_{13} cluster without destroying the structural skeleton is 8, beyond which the structural transition will take place.

We put eight oxygen atoms in eight nonadjacent tetrahedrons of an icosahedral Ba_{13} cluster, forming a $Ba_{13}O_8$ cluster. The optimized structure is shown in Fig. 3(e). However, contrary to the expectation of Ref. [6], we found that the icosahedron skeleton has already been broken; the mean nearest-neighbor bond length among Ba atoms decreases further to 4.170 Å, and the symmetry for a structural skeleton composed of 13 Ba atoms changes to C_s from I_h in the icosahedron. This is the reason that no high peak is found for a $Ba_{13}O_8$ cluster in the mass spectra [6]. Why can a high content of oxygen destroy the structure? To illustrate this, we calculated a $Ba_{13}O_2$ cluster, and found that in a stable structure the two oxygen atoms are positioned as far apart as possible, as shown in Fig. 3(f), which is in agreement with the expectation that it is not preferable for two oxygen atoms to be adjacent [6]. If there is too much oxygen, the strong interaction will destroy the structure of the cluster. In fact, the maximum number of oxygens in a Ba_{13} cluster is three [6] or four [28], but not eight, which is completely different from the cases of Fe(Co, Ni) oxide clusters. It was found that $M_{13}O_8$ and M_9O_6 are magic for M = Fe, Co, and Ni [29–31]. One possible reason for this difference is the magnetic interactions, which is absent in Ba oxide clusters.

IV. SUMMARY

By using an *ab initio* ultrasoft pseudopotential scheme combined with a molecular-orbital method, the structures of magic Ba clusters and Ba suboxide clusters were studied. The growth mechanism for a Ba cluster was discussed, and the effect of oxygen on Ba cluster structures was analyzed. The following conclusions were obtained: (1) Small Ba clusters grow in an icosahedral mode, which is induced by $5d$-electron bonding. (2) Due to the large atomic size of Ba, there are large cavities in magic Ba clusters, which make the magic Ba clusters able to trap O atoms. A small number of oxygen atoms can sustain the structural skeleton, which is why barium suboxide clusters can have the same magic numbers as pure barium clusters [6,28]. However, the polyicosahedron structural skeleton will be destroyed if the content of oxygen is too high. This study will shed some light on the bonding features of divalent metal clusters.

ACKNOWLEDGMENTS

The authors would like to express their sincere thanks to Dr. G. Kresse for his great help in our calculations, to Dr. Vijay Kumar and Dr. I. Boustani for discussions, and to the Materials Information Science Group of the Institute for Materials Research, Tohoku University, for their continuous support of the HITAC S-3800/380 supercomputing facility.

[1] R. Kawai and J.H. Wear, Phys. Rev. Lett. **65**, 80 (1993).
[2] V. Kumar and R. Car, Phys. Rev. B **44**, 8243 (1991).
[3] W.D. Knight, K. Clemenger, W.A. Heer, W.A. Saunder, M.Y. Chou, and M.L. Cohen, Phys. Rev. Lett. **52**, 2141 (1984).
[4] C. Bréchignac, Ph. Cahuzac, N. Kébaïli, J. Leygnier, and H. Yoshida, Phys. Rev. B **61**, 7280 (2000).
[5] D. Rayane, P. Melinon, B. Cabaud, A. Hearau, B. Tribolte, and M. Broyer, Phys. Rev. A **39**, 6056 (1989).
[6] V. Boutou, M.A. Lebeault, A.R. Allouche, C. Bordas, F. Pauling, J. Viallon, and J. Chevaleyre, Phys. Rev. Lett. **80**, 2817 (1998).
[7] J. Farges, M.F. Deferaudy, B. Raoult, and G. Torchet, Surf. Sci. **156**, 370 (1985).
[8] V. Boutou, A.R. Allouche, F. Spiegelmann, J. Chevaleyre, and M.A. Frcon, Eur. Phys. J. D **2**, 63 (1998).
[9] P. Lievens, P. Thoen, S. Bouckaert, W. Bouwen, F. Vanhoutte, H. Weidele, and R.E. Silverans J. Chem. Phys. **110**, 10 316 (1999).
[10] N. Malinowski, H. Schabler, T. Bergmann, and T.P. Martin, Solid State Commun. **69**, 733 (1989).
[11] T. Bergmann, H. Limberger, and T.P. Martin, Phys. Rev. Lett. **60**, 1767 (1988).
[12] T. Bergmann and T.P. Martin, J. Chem. Phys. **90**, 2848 (1989).
[13] G. Kresse and J. Hafner, J. Phys.: Condens. Matter **6**, 8245 (1994).
[14] G. Kresse and J. Hafner, Phys. Rev. B **47**, 558 (1993); **49**, 14 251 (1994).
[15] G. Kresse and J. Furthmüller, Phys. Rev. B **54**, 11 169 (1996).
[16] N.D. Mermin, Phys. Rev. A **137**, 1141 (1965).
[17] *CRC Handbook of Chemisty and Physics*, edited by D. R. Lide (CRC Press, New York, 1999), PP. 9-19–9-23.
[18] M.C. Payne, M.P. Teter, D.C. Allan, T.A. Arias, and J.D. Joannopoulos, Rev. Mod. Phys. **64**, 1045 (1992).
[19] D.M. Ceperley and B.J. Alder, Phys. Rev. Lett. **45**, 566 (1980).
[20] J.P. Perdew and A. Zunger, Phys. Rev. B **23**, 5048 (1981).
[21] G. Bergman, J.L.T. Waugh, and L. Pauling, Acta Crystallogr. **10**, 254 (1957).
[22] I. Boustani, A. Rubio, and J.A. Alonso, Chem. Phys. Lett. **311**, 21 (1999).
[23] E.K. Parks, L. Zhu, J. Ho, and S.J. Riley, J. Chem. Phys. **100**, 7206 (1994); **102**, 7377 (1995).
[24] J.M. Montejano-Carrizales, M.P. Iniguez, J.A. Alonso, and M.J. López, Phys. Rev. B **54**, 5961 (1996).
[25] M. Sakurai, K. Watanabe, K. Sumiyama, and K. Suzuki, J. Chem. Phys. **111**, 235 (1999).

[26] Q. Sun, X.G. Gong, Q.Q. Zheng, D.Y. Sun, and G.H. Wang, Phys. Rev. B **54**, 10 869 (1996).
[27] D.E. Ellis and G.S. Painter, Phys. Rev. B **2**, 2887 (1970).
[28] T.P. Martin and T. Bergman, J. Chem. Phys. **90**, 6664 (1989).
[29] Q. Wang, Q. Sun, M. Sakurai, J.Z. Yu, B.L. Gu, K. Sumiyama, and Y. Kawazoe, Phys. Rev. B **59**, 12 672 (1999).
[30] Q. Sun, Q. Wang, K. Parlinski, J.Z. Yu, Y. Hashi, X.G. Gong, and Y. Kawazoe Phys. Rev. B **61**, 5781 (2000).
[31] Q. Sun, M. Sakurai, Q. Wang, J. Z. Yu, G. H. Wang, K. Sumiyama, and Y. Kawazoe, Phys. Rev. B **62**, 8500 (2000).